Electrochemical and Solid-State Letters, **8** (10) A495-A499 (2005)
1099-0062/2005/8(10)/A495/5/$7.00 © The Electrochemical Society, Inc.

Electrochemical Capacitor of $MnFe_2O_4$ with NaCl Electrolyte

Shin-Liang Kuo and Nae-Lih Wu*,z

Department of Chemical Engineering, National Taiwan University, Taipei, Taiwan 106

Ferrites including MFe_2O_4 where M = Mn, Fe, Co, or Ni have been synthesized by solution methods and tested for their capacitive behaviors in aqueous NaCl solution. $MnFe_2O_4$ has been found to exhibit unusually large capacitances, while the other ferrites do not. The results indicate unique pseudocapacitive property associated with the Mn^{+2} ions at the tetrahedral sites in the spinel structure. The pseudocapacitance was observed only for crystalline, rather than amorphous, $MnFe_2O_4$ phase, which has exhibited specific capacitances of >100 F/g and high-power delivering capabilities of >10 kW/kg.
 [DOI: 10.1149/1.2008847]

Manuscript submitted April 14, 2005; revised manuscript received June 4, 2005. Available electronically August 4, 2005.

Electrochemical capacitors are promising energy storage devices for meeting the high-power electric market.[1-3] Complementary to battery, electrochemical capacitors can provide superior power density and cyclability, and can be regarded as an intermediate device between the traditional ceramic capacitors and batteries. Electrochemical capacitors are generally categorized into two types based on the charge-storage mechanism. The electric double-layer capacitance (EDLC) arises from electrostatic separation of charges at the interface between electrode and electrolyte. On the other hand, pseudocapacitance, typically more than ten times greater than EDLC, results from either superficial or multi-electron-transfer faradaic reactions with fast charge/discharge properties.

Although hydrated amorphous ruthenium oxide, $RuO_2{\cdot}xH_2O$, has demonstrated high specific capacitance and power-density in aqueous H_2SO_4,[4-6] its extraordinary cost limits potential commercial applications. Therefore, much research has been focused on the development of pseudocapacitive materials of lower cost. MnO_2, because of its low cost and environmental benignity, has drawn much attention recently.[7-11] Lee and Goodenough[7,8] first reported that amorphous manganese oxide (a-$MnO_2{\cdot}nH_2O$) particles synthesized via reduction of potassium permanganate exhibits a capacitance of ca. 200 F/g. Although higher capacitances have been reported for the thin-film type of electrodes,[9-11] they are unlikely to be commercially viable because of their slow process throughput. The pseudocapacitance of MnO_2 is believed to result from multielectron transfer at Mn cation sites, balanced by intercalation/extraction of cations within the oxide structure.[7,8] Note that it is the amorphous phase that exhibits the largest capacitance, and dramatic reduction in capacitance occurs with increasing crystallinity.

Fe_3O_4 is another recently discovered inexpensive electrode material, exhibiting pseudocapacitance with alkali sulfites and sulfates electrolytes.[12-14] Its capacitance, ranging from 30 to 510 F/g,[12] has been found to be very sensitive to the electrolyte anion species and the dispersion of the oxide crystallites. There are also known several ferrites bearing the same general formula, MFe_2O_4, as and similar crystal structures to Fe_3O_4 (or $FeFe_2O_4$). This study was originally motivated to investigate the capacitive behaviors of these ferrite materials. In brief, among $MnFe_2O_4$, Fe_3O_4, $CoFe_2O_4$, and $NiFe_2O_4$, $MnFe_2O_4$ was found to exhibit unusually large capacitances in NaCl electrolyte, and its capacitive characteristics suggest a pseudocapacitance mechanism completely different from that of Fe_3O_4 but close to that of MnO_2. This new pseudocapacitive ferrite exhibits favorable properties for high-power applications.

Experimental

Ferrites, including MFe_2O_4, where M = Mn, Fe, Co, or Ni, were synthesized via a precipitation technique in basic aqueous solutions as follows. Either MCl_2 (M = Fe, Co, and Ni) or $MnSO_4$ was dissolved along with $FeCl_3$ with a stoichiometric ratio of 2:1 in 1 M HCl aqueous solution with bubbling N_2. When the solution was added with a 1.5 M NaOH solution under vigorous stirring, either black or dark-brownish precipitate was formed immediately. Once the precipitate sedimented, the supernatant liquid was decanted and fresh deionized water was added. The consecutive solution-decanting and water-replenishing processes were carried out to remove residual ions. The powder was prepared by drying the precipitate at 50°C. A subsequent calcination process was carried out at different temperatures for 2 h in N_2 atmosphere.

Ferrite/carbon black (CB; VULCAN X72, Cabot Corp., U.S.A.) composite powders with a weight ratio of 1:1 between the two component have also been synthesized via a similar process except that the CB powder was introduced in the starting aqueous solution prior to the precipitation step. It was found that all the CB precipitated simultaneously with the oxide precursor, suggesting that the oxide component was homogeneously combined with the CB particles during the synthesis process.

Powder X-ray diffraction (XRD) was performed on MacScience/MXP diffractometer with Cu Kα radiation ($\lambda = 0.15418$ nm), while synchrotron XRD ($\lambda = 0.061993$ nm) was performed using the beam-line 01-C2 facilities of National Synchrotron Radiation Research Center in Taiwan. Micrographs were taken on a scanning electron microscope (Hitachi-S800). Brunauer-Emmett-Teller (BET) surface areas were determined by nitrogen adsorption (ASAP 2000, Micrometrics).

Two types of electrodes have been prepared for characterization. The first type, referred to as the "mixed" electrode, consists of the ferrite particles and the CB powder with a weight ratio of 9:1 mixed by mechanical grinding. The second type, referred to as the "coprecipitated" electrode, was made of the ferrite/CB composite powders. PVdF in 10 wt % was used as the binder for both electrodes and Ti foil was used as the current collector. The electrodes were finally dried at 120°C for 6 h in vacuum.

Electrochemical characterizations were carried out with a three-electrode cell with Pt mesh and Ag/AgCl/saturated KCl (EG&G, 197 mV vs NHE at 25°C) as the counter and reference electrode, respectively. The electrolyte solution was 1 M NaCl aqueous solution, unless otherwise specified. The cyclic voltammetry was recorded by an electrochemical analyzer (Eco Chemie PGSTAT30). The average specific capacitance of the electrodes was calculated by

$$C_{avg} = \Delta Q/w\Delta V = \left(\int IdV\right)/s/\Delta V/w \qquad [1]$$

where ΔQ is the total amount of charge accumulated over a potential window ΔV, w is the mass of active material in an electrode, I is the current, and s is the potential scan rate.

Results and Discussion

Figure 1 shows the powder XRD patterns of the synthesized ferrites, including $MnFe_2O_4$, Fe_3O_4, $CoFe_2O_4$, and $NiFe_2O_4$. All the powders are single-phased, exhibiting spinel structure having the same space group, O_h^7-$Fd3m$. These ferrites show different crystallization ability. Fe_3O_4 is the only one that is capable of fully crys-

* Electrochemical Society Active Member.
z E-mail: nlw001@ntu.edu.tw

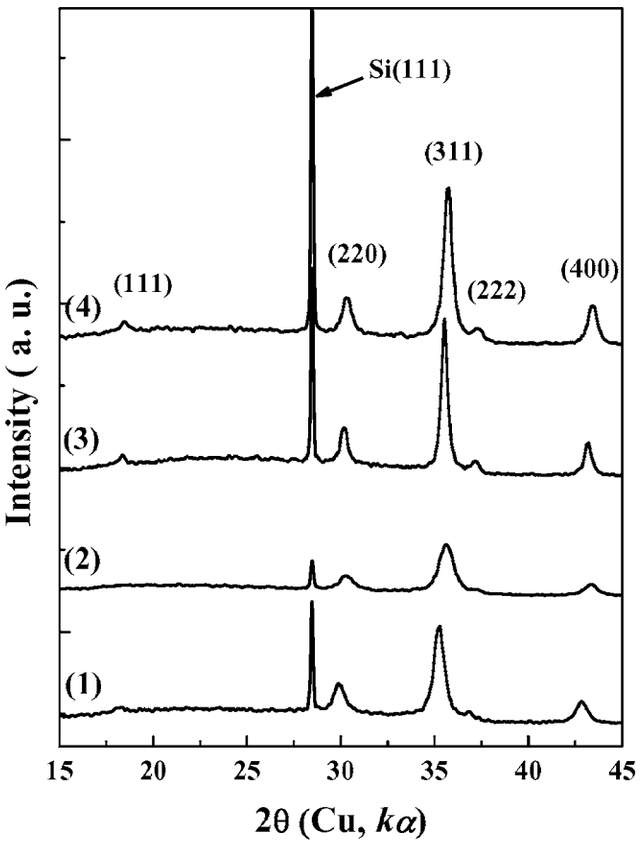

Figure 1. XRD patterns of MFe_2O_4. (1) $MnFe_2O_4$ calcined at 600°C, (2) Fe_3O_4 without calcination, (3) $CoFe_2O_4$, 600°C, and (4) $NiFe_2O_4$, 600°C. Si is used as the internal standard, and the plane indices of the ferrites are given based on the spinel structure.

tallizing during the precipitation process in solution, and it shows an average crystallite size of 9.5 nm, as determined by Debye-Scherrer equation based on the (311) diffraction peak (Table I). On the other hand, the other ferrites were amorphous as precipitated and subsequently crystallized during calcination in N_2 at elevated temperatures. The crystallite sizes of the ferrite powders calcined at 600°C are listed in Table I. Scanning electron microscopy (SEM) images (Fig. 2) show that the ferrite powders contain granular particles with fairly uniform diameters of about 50 nm. No apparent difference in either particle size or morphology among these samples was observed. The particle sizes are larger than the crystallite sizes determined from XRD, suggesting that the particles are composed of several crystallites.

For electrochemical characterization, a control study was first carried out on the Ti current collector and CB, respectively. As described earlier, CB was used as a conducting additive in the ferrite

Table I. The microstructural and electrochemical data of single-phased ferrite powders.

Sample	Calcination (°C)	Crystallite size (nm)	BET (m^2/g)	Specific capacitance (F/g-MFe_2O_4)	Specific capacitance ($\mu F/cm^2$)
$MnFe_2O_4$	600	21.5	23.2	14.9	64.4
Fe_3O_4	50	9.5	97.9	1.2	1.2
$CoFe_2O_4$	600	25.0	30.2	7.1	23.5
$NiFe_2O_4$	600	16.4	33.6	<3.0	<1.0

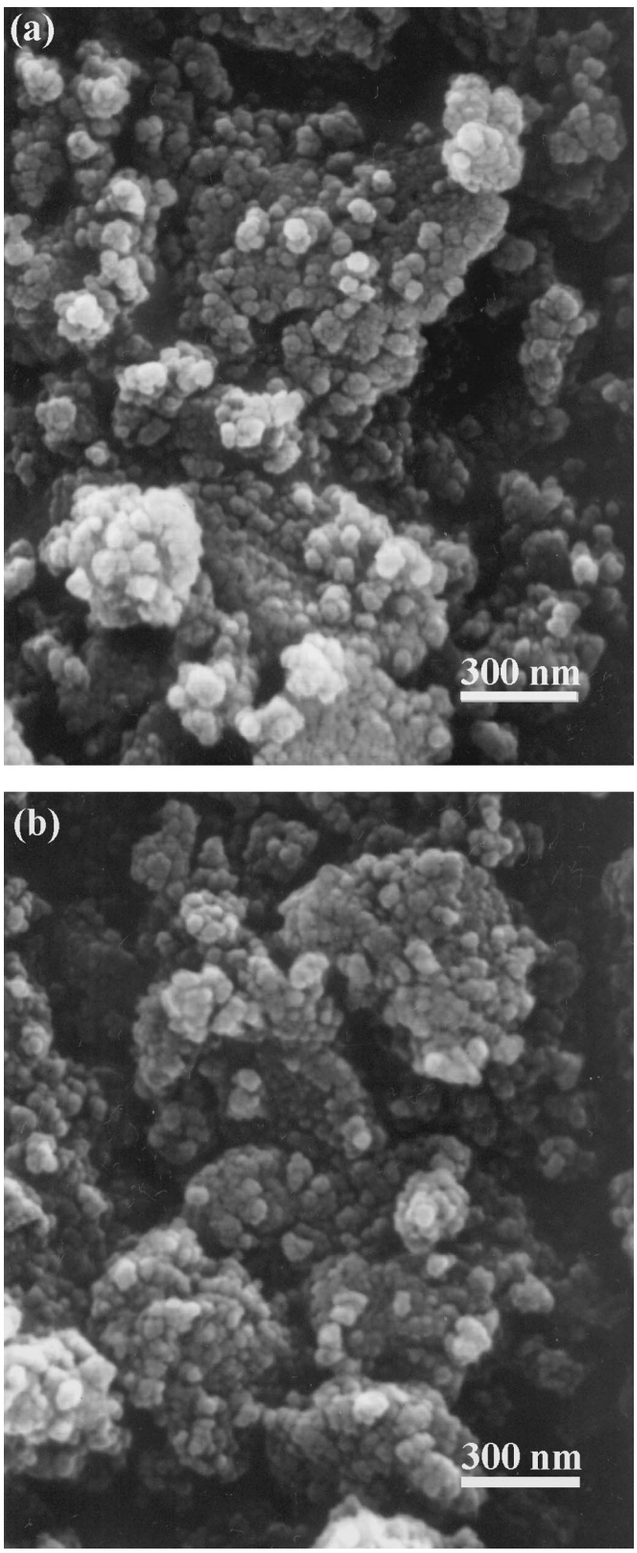

Figure 2. SEM images of ferrites (a) $CoFe_2O_4$ and (b) $MnFe_2O_4$ calcined at 600°C.

electrodes. For Ti foil (Fig. 3), only reduction of H^+ and oxidation of OH^- occur at −0.2 and 1.05 V, respectively. On the other hand, CB electrode exhibits a nearly rectangular current profile, characteristic of EDLC (Fig. 3), within the potential window of the Ti current

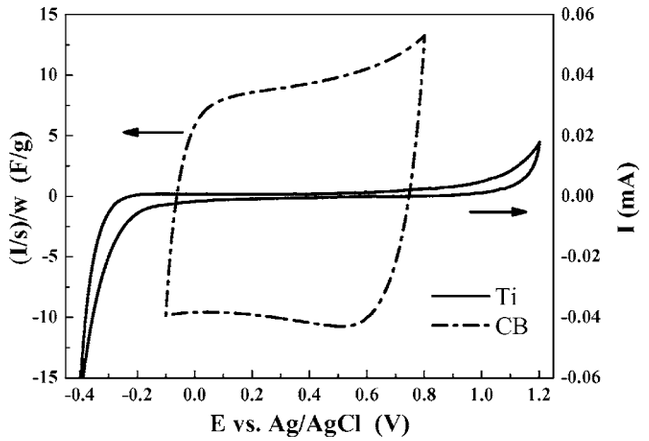

Figure 3. CVs of the electrodes operating in 1 M $NaCl_{(aq)}$, (——) Ti foil, and (—·—·) carbon black electrode.

collector, and it shows a specific capacitance of ~10 F/g. As the CB powder has a specific surface area of nearly 200 m^2/g, this gives a superficial specific capacitance of about 5 $\mu F/cm^2$. This capacitance is lower than that, ca. 10 ~ 20 $\mu F/cm^2$, reported in $H_2SO_{4(aq)}$ electrolyte.[15] This may be because the ions in the present electrolyte solution have larger radii than proton, and a part of surface area within micropores of CB becomes inaccessible.

Figure 4 compares the voltammograms of the mixed electrodes for each of the ferrite powders that have been calcined at 600°C. Apparently, these ferrites exhibit very different capacitive behaviors in aqueous NaCl. The average capacitances of the electrodes have been calculated from Eq. 1 within the integrated potential range between 0.0 and 0.7 V (to disregard the transition regions upon reversal of potential-scan), and the capacitances due to the ferrites were estimated by subtracting the contribution of CB, which is ~1.0 F per gram of the mixture of ferrite and CB. As summarized in Table I, $NiFe_2O_4$ and Fe_3O_4 exhibit negligible (<3.0 F/g) capacitances. $CoFe_2O_4$ provides a moderate gravimetric specific capacitance up to 7.1 F/g, while $MnFe_2O_4$ shows the largest capacitance of 14.9 F/g with a fairly rectangular current profile (Fig. 4). Taking into account of the BET surface area data of the ferrite

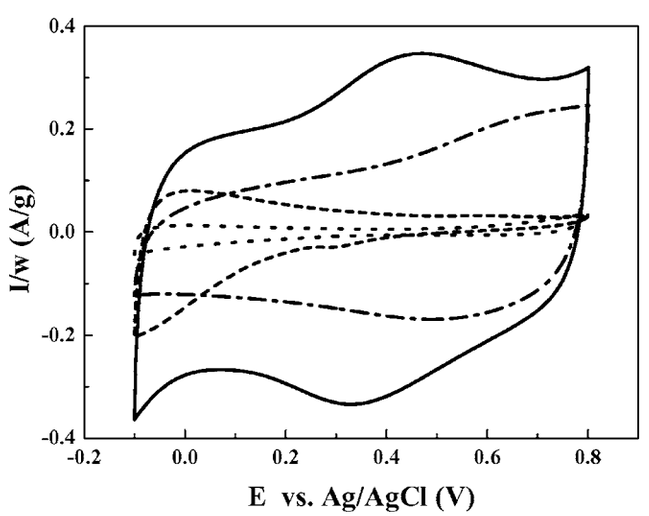

Figure 4. CVs of the mixed electrodes operating in 1 M aqueous NaCl electrolyte: (·····) $NiFe_2O_4$, (---) Fe_3O_4, (—·—·) $CoFe_2O_4$, and (———) $MnFe_2O_4$. (Scan rate: 20 mV/s.)

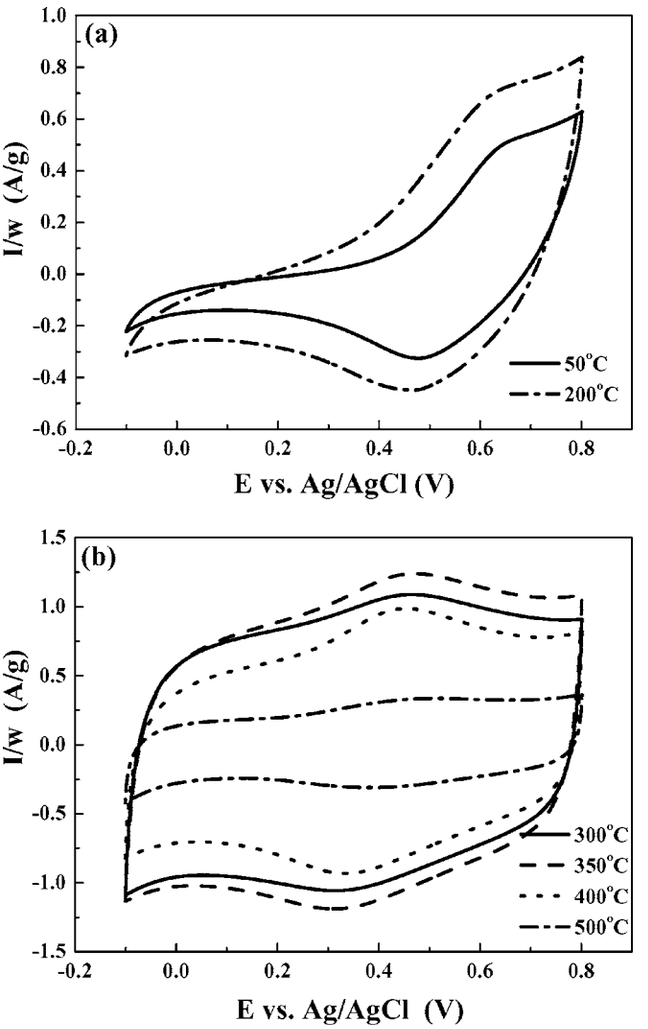

Figure 5. CVs of the coprecipitated electrodes constituted of the $MnFe_2O_4$/carbon black powders calcined at different temperatures: (a) 50 and 200°C, (b) 300, 350, 400, and 500°C. (Scan rate 20 mV/s.)

particles (Table I) gives superficial specific capacitances of 23.5 and 64.4 $\mu F/cm^2$ for $CoFe_2O_4$ and $MnFe_2O_4$, respectively. The latter is more than ten times that of CB. As shown below, the capacitance of $MnFe_2O_4$ can be further enhanced by lowering the calcination temperature.

Figures 5a and b show the voltammograms of the coprecipitated electrodes which are constituted of the coprecipitated $MnFe_2O_4$/CB composite powders calcined at different temperatures ranging from 50 to 500°C. The electrodes can be divided into two categories based on their capacitive behaviors. Powders calcined at or below 200°C do not give capacitive current profiles (Fig. 5a), while those calcined at or above 300°C result in rectangle-shaped current profiles (Fig. 5b), characteristic of capacitors. For the latter, the specific capacitances were again calculated from Eq. 1 with integrated potential range between 0.0 and 0.7 V, and the contribution of CB (~5 F/g-composite) was subtracted. As shown in Table II, the specific capacitance of the $MnFe_2O_4$ component first increase and then decrease with increasing calcination temperature, showing the maximum of 102.4 F/g-$MnFe_2O_4$ for calcination at 350°C. As described below, the XRD crystallite size of this $MnFe_2O_4$ powder is 13.2 nm (Table II), and its specific surface area was estimated to be no greater than 91 m^2/g, which corresponds to the specific surface area of nonagglomerated crystallites. This gives a superficial capacitance

Table II. The microstructural and electrochemical data of $MnFe_2O_4$ in the $MnFe_2O_4$/carbon black composite powders.

Sample	Calcination (°C)	Crystallite size (nm)	Specific capacitance (F/g-composite)	Specific capacitance (F/g-$MnFe_2O_4$)
1	50	-	Noncapacitive	Noncapacitive
2	200	-	Noncapacitive	Noncapacitive
3	300	2.5	50.6	91.2
4	350	13.2	56.2	102.4
5	400	17.6	41.6	73.2
6	500	23.2	14.8	19.5

of at least 112 $\mu F/cm^2$ for the 350°C calcined $MnFe_2O_4$ crystallites. This value is much larger than that (64.4 $\mu F/cm^2$) of the mixed electrode of $MnFe_2O_4$, and the reasons may be of several folds. For one, the coprecipitation approach may allow the ferrite crystallites to be better dispersed and/or in more close contact with the conductive CB component as compared with physical grinding. For another, the capacitance in the mixed electrode may be limited by the lack of electrolyte ions, as pointed out by Zheng[5] for ruthenium oxide electrodes, and the additional CB in the coprecipitated electrode could serve as an electrolyte reservoir to provide sufficient electrolyte ions. The optimum CB content has yet to be determined.

By gradually increasing the potential-scan range, it is determined that the $MnFe_2O_4$/CB electrode has a practical operating potential range that is identical to that of the Ti current collector shown in Fig. 3. Another important property of this electrode is that it is capable of delivering rather high capacitance under high-power conditions. Figure 6 shows the CVs of a two-electrode cell of the coprecipitated $MnFe_2O_4$/CB electrodes. The capacitive current (at 0.0 V) is found to decrease by merely 22% when the potential-scan rate increases by a factor of 10, from 20 to 200 mV/s. At 200 mV/s, the composite electrode delivers a maximum specific power of 8.7 kW/kg composite. By subtracting the contribution from CB as described before, the $MnFe_2O_4$ component was found to deliver 15.4 kW/kg-$MnFe_2O_4$.

Synchrotron XRD analysis (Fig. 7) shows that the powder is essentially amorphous after calcination at 200°C. On the other hand, all the important reflections of $MnFe_2O_4$ began to appear after calcination at 300°C, above which the peaks of the ferrite phase were increasingly sharpened, suggesting crystal growth, with increasing calcination temperature. The average crystallite sizes are listed in Table II. These results indicate that the abrupt change in capacitive behavior as observed between powders calcined at 200 and 300°C is associated with the formation of crystalline $MnFe_2O_4$. That is, it is crystalline $MnFe_2O_4$ that is responsible for the large capacitance. The further increase in capacitance from 300 to 350°C can thus be attributed to improved crystallinity of existing $MnFe_2O_4$ crystallites, while the subsequent decline in capacitance at higher temperatures is due to loss in surface area of the crystallites caused by crystal coarsening and sintering.

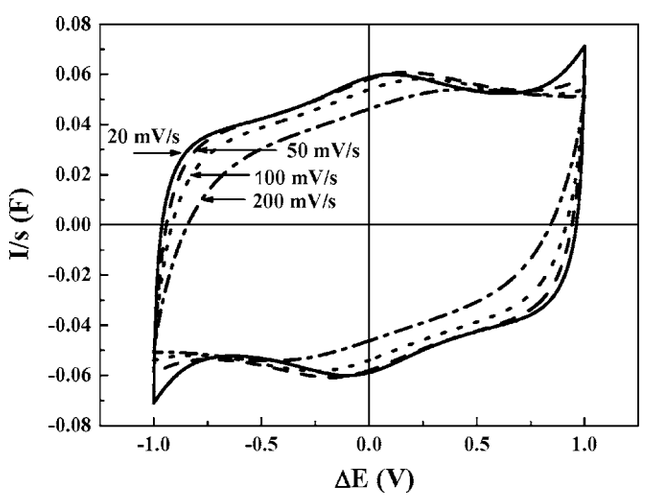

Figure 6. CVs acquired at different scan rates for the coprecipitated electrode that is constituted of the $MnFe_2O_4$/carbon black powders calcined at 350°C.

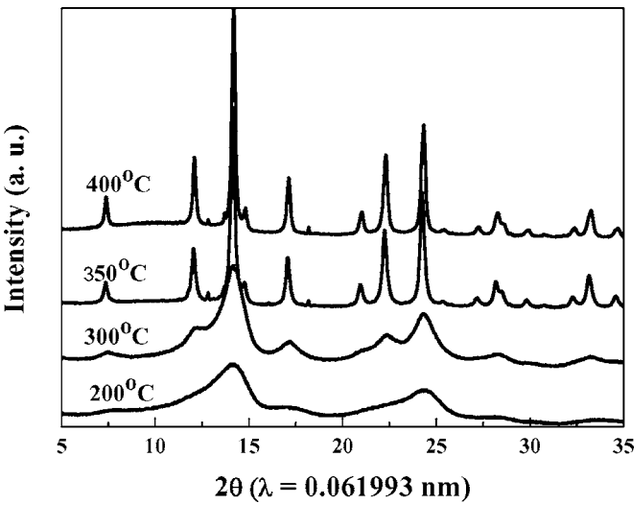

Figure 7. XRD patterns of the coprecipitated MFe_2O_4/carbon black powders calcined at different temperatures.

The CVs of both the mixed and coprecipiated $MnFe_2O_4$ electrodes showed a couple of broad humps (Fig. 4 and 5b), indicative of the occurrence of some sort of faradaic reactions. That is, the unusually large capacitance exhibited by $MnFe_2O_4$ is pseudocapacitance in nature. From the comparison among different ferrites shown in Table I, it is clear that Mn ion must play an important role in causing the pseudocapacitive behaviors. $MnFe_2O_4$ is known to have a normal spinel structure where Mn^{+2} ions predominantly occupy the tetrahedral sites surrounded by O^{2-}. This is in contrast to the other ferrites shown in Table I, which have the inverse spinel structure with the corresponding divalent ions, including Ni^{+2}, Co^{+2}, and Fe^{+2}, occupying the octahedral sites. It is also worth mentioning that, although not shown, $MnFe_2O_4$ has also been found to exhibit large capacitances in K^+-containing electrolytes as well. This is very similar to the case of pseudocapacitance of MnO_2, which is known to result from electron-transfer at the Mn ions balanced by intercalation of cations, namely Na^+ and K^+.[7,8] It is conjectured at this point that the pseudocapacitance of $MnFe_2O_4$ might involve a similar mechanism. However, the major difference is that such reactions are feasible even when MnO_2 is amorphous, but in the ferrite, the electron-transfer process appears possible only by the particular environment associated with the tetrahedral sites in the spinel structure. Clearly further research is needed to unequivocally unravel the pseudocapacitance mechanism.

Conclusion

Among ferrites MFe_2O_4 where M = Mn, Fe, Co, and Ni, $MnFe_2O_4$ has been found to exhibit pseudocapacitance in aqueous NaCl solution, while the other ferrites do not. Crystallographic and electrochemical data indicate that the unusually large capacitances result from the crystalline, rather than amorphous, $MnFe_2O_4$ phase, which has shown a gravimetric specific capacitance greater than 100 F/g, or a superficial capacitance of at least 112 $\mu F/cm^2$, with an operating window of nearly 1.2 V and high-power delivering capability. The pseudocapacitive behavior is suggested to arise from

electron-transfer at the Mn ions at the tetrahedral sites of the spinel, balanced by intercalation of cations, such as Na^+ and K^+, from the electrolyte.

Acknowledgment

This work is supported by National Science Council of Republic of China under contract no. NSC 93-2214-E-002-015.

National Taiwan University assisted in meeting the publication costs of this article.

References

1. B. E. Conway, *J. Electrochem. Soc.*, **138**, 1539 (1991).
2. B. E. Conway, V. Briss, and J. Wojtowicz, *J. Power Sources*, **66**, 1 (1997).
3. R. Kötz and M. Carlen, *Electrochim. Acta*, **45**, 2483 (2000).
4. J. P. Zhang, P. J. Cygan, and T. R. Jow, *J. Electrochem. Soc.*, **142**, 2699 (1995).
5. J. P. Zheng, *Electrochem. Solid-State Lett.*, **2**, 359 (1999).
6. J. P. Zheng and T. R. Jow, *J. Power Sources*, **62**, 155 (1996).
7. H. Y. Lee and J. B. Goodenough, *J. Solid State Chem.*, **144**, 220 (1999).
8. H. Y. Lee, V. Manivannan, and J. B. Goodenough, *C.R. Acad. Sci., Ser. IIc: Chim*, **1999**, 565.
9. R. N. Reddy and R. G. Reddy, *J. Power Sources*, **124**, 330 (2003).
10. C. C. Hu and T. W. Tsou, *Electrochem. Commun.*, **4**, 105 (2002).
11. S.-C. Pang, M. A. Anderson, and T. W. Chapman, *J. Electrochem. Soc.*, **147**, 444 (2000).
12. N. L. Wu, Y. P. Lan, C. Y. Han, S. Y. Wang, and L. R. Shiue, Abstract 212, The Electrochemical Society Meeting Abstract, Philadelphia, PA, USA, May 12–17, 2002.
13. N. L. Wu, S. Y. Wang, C. Y. Han, D. S. Wu, and L. R. Shiue, *J. Power Sources*, **113**, 173 (2003).
14. S. Y. Wang and N. L. Wu, *J. Appl. Electrochem.*, **33**, 345 (2003).
15. G. Salitra, A. Soffer, L. Eliad, Y. Cohen, and D. Aurbach, *J. Electrochem. Soc.*, **147**, 2486 (2000).